Preferred citation: A.-L. Erkkilä, T. Leppänen, J. Sorvari and T. Tuovinen. Prediction of curl behaviour. In **Advances in Pulp and Paper Research, Oxford 2017**, *Trans. of the XVIth Fund. Res. Symp. Oxford, 2017*, (W. Batchelor and D. Söderberg, eds), pp 43–68, FRC, Manchester, 2018.
DOI: 10.15376/frc.2017.1.43.

PREDICTION OF CURL BEHAVIOUR

A.-L. Erkkilä[1], T. Leppänen[2], J. Sorvari[3] and T. Tuovinen[1]

[1] University of Jyväskylä, P.O. Box 35, FI-40014 Jyväskylä, Finland
[2] LUT Savo Sustainable Technologies, Lappeenranta University of Technology, Varkaus unit, Opiskelijankatu 3, FI-78210 Varkaus, Finland
[3] Centre of Computational Engineering and Integrated Design (CEID), Lappeenranta University of Technology, P.O. Box 20, FI-53851 Lappeenranta, Finland

ABSTRACT

Curl is unwanted dynamic behaviour that appears already in the manufacturing process and evolves through the end-use of paper or board due to moisture content changes and mechanical treatments. In this paper, the analytical and numerical approaches are used to reveal the sensitivity of the curl tendency to fundamental variables affecting deformation behaviour of paper. Good agreement between the measured curvatures induced into the sheet by the photocopying process and the simulated curvatures is achieved. Paper is treated as a multi-layered material, and finite element simulations are performed by using hygro-elasto-plastic and hygro-viscoelastic material models. Also analytical calculations are carried out to support the conclusions. The results show that the prediction and control of curl is not straightforward; curl depends not only on the fibre orientation structure but interacts in a complex way with the through-thickness dry solids content profiles during moisture content changes and external mechanical forces acting on paper. Despite the complexity of the phenomenon, the simplified computational approaches presented in this paper can be used for analysing and optimising the paper structure and process parameters to prevent detrimental curl.

1 INTRODUCTION

The curl of paper or board is a common problem from production to end use. Research on curl was initiated already in the 1950s by Smith [1], and it has continued since then for nearly seven decades. During these decades, several

factors affecting the curl tendency have been studied, and especially the importance of drying [1] and fibre orientation two-sidedness [2, 3] has been manifested. After the pioneering studies, the effect of these factors on the curl tendency has been clarified by several authors. Carlsson *et al.* [4] and Carlsson [5] have introduced an equation for curvature which has also been utilised for local curls by Leppänen and Hämäläinen [6]. The time-dependent behaviour of curl has been studied by Uesaka *et al.* [7] and Lu and Carlsson [8]. An apparatus for curl and twist measurements has been presented by Eriksson *et al.* [9], and a commercial 3D laser scanner system has been used by Decker *et al.* [10]. Viitaharju and Niskanen [11] have studied the effect of microfibrils on the diagonal curl, and the effect on the initial deflections on curl has been studied by Lu and Carlsson [12]. Hirn and Bauer [13] have examined the effects of the two-sidedness of the fibre orientation angle and fibre orientation anisotropy on curl behaviour. Bortolin *et al.* [14] have introduced a grey-box model for the curl and twist of carton board, and an automatic measurement and control system for fibre orientation has been applied for a paper machine to reduce the twist-curl [15].

In the latest decades, the finite element method has been applied in several curl studies with elastic [12, 16], viscoelastic [7, 8] and elasto-plastic [17, 18] material models. In this paper, finite element analysis and analytical curl tendency calculations are used to show the importance of the concurrent effect of the through-thickness variation of the fibre orientation and the in-plane tensions and through-thickness dry solids content profiles during moisture content changes. Results are obtained with the hygro-elasto-plastic material model and the hygro-viscoelastic approach, and analytical curl calculations are used to complete the general view. The results of the elasto-plastic simulations are also compared with the measured curl induced by photocopying.

2 MEASUREMENTS AND MODELS

2.1 Measurements

The curl tendency after photocopying and the layered fibre orientation structure of seven 75 g/m^2 fine paper samples were determined. The samples were produced by the same production machine, but the wet end process parameters were altered to attain different fibre orientation distribution structures throughout the paper thickness. The fibre orientation distribution of the sample layers was determined from the scanned layer images [19, 20] and defined by the orientation angle θ (°) and the anisotropy ξ (–) [17]. The orientation angle describes the deviation of the main direction of the fibre orientation distribution from the machine direction (MD). Orientation angles θ counterclockwise from

the MD are defined as positive when viewed from the top side. Anisotropy ξ is a ratio of the main and the minor axis of the distribution, see Figure 8 (upper left). The fibre orientation structures of the seven samples considered are presented in Figure 1.

The curl measurements conducted after processing the samples in a photocopier device followed the standard ISO 14968:1999. A4 sheets for the curl tests were collected from the cross-profile position identical with the fibre orientation analysis. One-sided copying was processed either on the bottom or on the top side of the sheets and packs of 10 to 15 consecutive copied sheets were then pulled from middle of the stack for the measurement of curl curvature parameters K_{MD} and K_{CD}. Curl curvatures K are reciprocal to the radii of arc of sheet edges in the unit 1/m, and they are measured comparing the arc of sheet pack edges with the curl gauge (see ISO 14968:1999). K_{MD} is measured from the edges of the sheet along the MD and K_{CD} from the edges of the sheet along the CD (cross direction). In this study, if the direction where the sheet edges rise, i.e. the concave side of the sheet, is toward the bottom side (BS), the sign of curvature K is negative, and if the concave side is toward the top side (TS), the curvature is marked with a positive sign. The curl of sheet may appear in different modes, i.e. the main axis of the cylindrical shape of the sheet may be along the MD ($K_{MD} = 0$), along the CD ($K_{CD} = 0$), or be manifested by a diagonal axis deviating from the main axis ($K_{MD} \neq 0$ and $K_{CD} \neq 0$ with the same signs), as seen in the example in Figure 8 (bottom right). In addition to the cylindrical shape, the curl may in some cases also be cup-shaped (signs of K_{MD} and K_{CD} are equal) or saddle-type (signs of K_{MD} and K_{CD} are different).

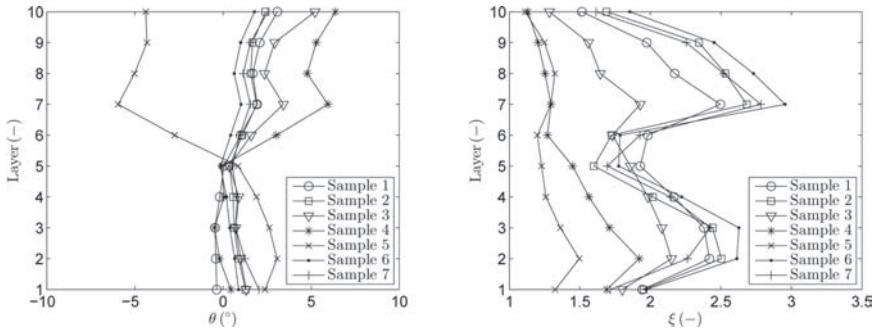

Figure 1. Layered fibre orientation angles (*left*) and anisotropies (*right*) measured from the production machine samples.

2.2 Models

Hygro-viscoelastic and hygro-elasto-plastic material models were used to predict the curl behavior of a paper sheet. The material was assumed to be isotropic in the viscoelastic approach and orthotropic in the elasto-plastic approach. However, the hygroexpansion strain depends on the anisotropy in both material models and also on the dry solids content (DSC) in the elasto-plastic material model. In both approaches, a plane stress state was assumed.

In the elasto-plastic approach, the dependence between stress $\sigma = (\sigma_1, \sigma_2, \sigma_{12})^\top$ and strain $\varepsilon = (\varepsilon_1, \varepsilon_2, \varepsilon_{12})^\top$ was defined by the generalised Hooke's law as

$$\sigma = C(\varepsilon - \beta \Delta c), \tag{1}$$

where C is the constitutive matrix, $\beta = (\beta_1, \beta_2, 0)^\top$ (%/%) is the moisture expansion coefficient and Δc (–) is the dry solids content change. The direction 1 coincides with the orientation angle and the direction 2 is perpendicular to the direction 1. The material parameters depend on the anisotropy and dry solids content, and are derived in detail in the references [21] and [22]. For the elasto-plastic material model the stress-strain dependency is defined using the equations based on experimental results

$$\sigma = \begin{cases} E\varepsilon & \text{if} \quad \varepsilon \le \varepsilon_y \\ E\varepsilon_y - \dfrac{H}{2E} + \sqrt{H\left(\dfrac{H}{4E^2} + \varepsilon - \varepsilon_y\right)} & \text{if} \quad \varepsilon > \varepsilon_y \end{cases}, \tag{2}$$

$$P = \left(A_1 + A_2\phi + A_3 c\right)^{1/n} \qquad P = \left\{\sigma_y, \varepsilon_y, H\right\}, \tag{3}$$

where $E = \sigma_y/\varepsilon_y$ (Pa) is the elastic modulus, ε_y is the yield strain, σ_y is the yield stress, H (Pa^2) is the hardening constant and c = [0, 1] is the dry solids content. In Eq. (3), P is any of the variables σ_y, ε_y or H and the parameters A_1, A_2, A_3 and n are the fitting constants, see Table 1, and the anisotropy index ϕ (–) is defined by the equation

$$\phi = \sqrt{\frac{1 - \xi^2}{\xi + \tan^2 \gamma / \xi}} + \xi, \tag{4}$$

where ξ (–) is the fibre orientation anisotropy and γ (rad) is the angle from the minor axis of the fibre orientation distribution [22]. Examples of the modelled

stress-strain behaviours and yield surfaces based on Hill's yield criterion are shown in Figures 2 and 3.

The moisture expansion coefficients β are defined by the equation

$$\beta = \frac{k\phi^v}{c^2}\exp\left(\frac{k\phi^v}{-\frac{1}{a}k\phi^v + \frac{b}{a}\left(1-\exp\left(-100\frac{k\phi^v}{a}\right)\right)}\left(\frac{1}{c}-1\right)\right), \tag{5}$$

where the fitting parameters have values $k = 0.0439$, $v = -0.9015$, $a = 2.5054$ and $b = 0.0250$ [21, 23]. Examples of the dry solids content and anisotropy dependent moisture expansion coefficients are shown in Figure 4.

The time-dependent curl behaviour was simulated by the linear viscoelastic material model

$$\varepsilon(t) = \int_0^t D(t-\tau)\dot{\sigma}(\tau)d\tau + \beta\Delta c, \tag{6}$$

where D (1/Pa) is the compliance matrix, t (s) is the time, τ (s) is the integration variable and $\dot{\sigma}(\tau) = (\dot{\sigma}_1(\tau), \dot{\sigma}_2(\tau), \dot{\sigma}_{12}(\tau))^\top$ (Pa/s) is the stress rate vector. Examples of the simulated creep curves are presented in Figure 5. For the viscoelastic model, the moisture expansion coefficients depend on the anisotropy, but not on dry solids content, see Table 2. A more detailed description of the viscoelastic material model is presented in reference [24].

Table 1. The fitting parameters of Eq. (3) for the yield stress σ_y, the yield strain ε_y and the hardening constant H [21]

	A_1	A_2	A_3	n
σ_y	–5.9030 (Pa^n)	3.1959 (Pa^n)	18.3077 (Pa^n)	0.1760 (–)
ε_y	380.4181 (–)	14.3408 (–)	–269.8327 (–)	–0.7720 (–)
H	–0.6021 (Pa^{2n})	4.0423 (Pa^{2n})	11.3795 (Pa^{2n})	0.0715 (–)

Table 2. Moisture expansion coefficients β_1 and β_2 for anisotropies 1.5, 2.0 and 2.5 used in the viscoelastic simulations. The coefficients were defined by Eq. (5) using dry solids content $c = 0.90$.

ξ (–)	β_1 (%/%)	β_2 (%/%)
1.5	2.53×10^{-2}	4.07×10^{-2}
2.0	2.12×10^{-2}	4.76×10^{-2}
2.5	1.83×10^{-2}	5.37×10^{-2}

2.3 Numerical simulations

A sample with a thickness of 0.100 mm and in-plane dimensions of 75 mm × 75 mm were used in the simulations. The simulations consist of five separate steps where the in-plane tensions and through-thickness dry solids content profiles are applied and removed. At the end of the simulations, no external in-plane tensions occur and a constant through-thickness dry solids content is assigned. The detailed procedure is the following:

Step 1: Initial constant dry solids content: elasto-plastic approach 85% and viscoelastic approach 87%. The out-of-plane deformation of the sample is restrained (displacement $u_3 = 0$ in all nodes). All displacements and rotations are restrained in the middle of the sample. External in-plane tensions (if any) are applied.

Step 2: One of the through-thickness dry solids content profiles presented in Figure 6 is applied into sample.

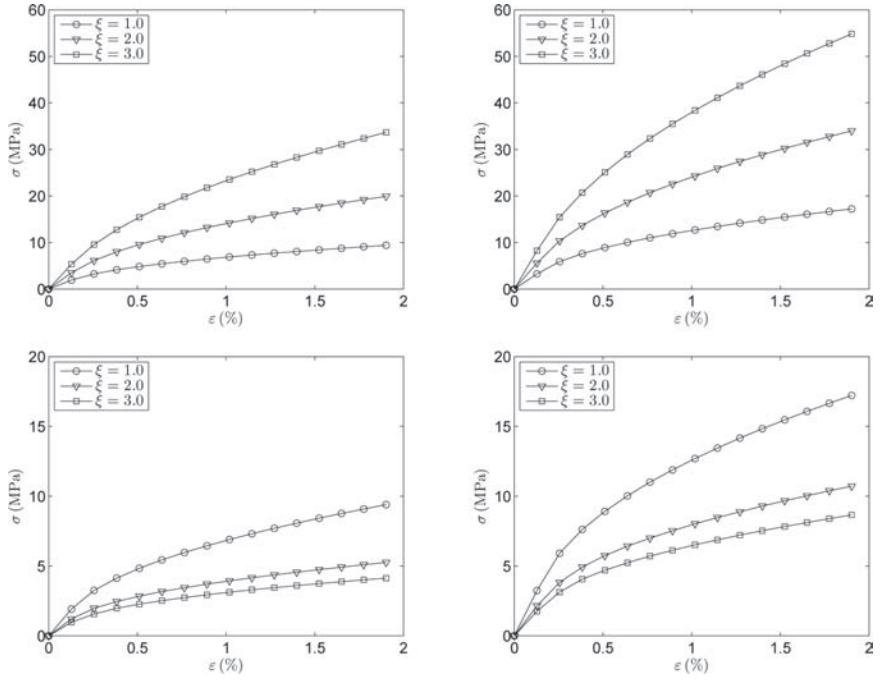

Figure 2. Examples of the stress-strain behaviour in the elasto-plastic approach for the main direction (*top*) and transverse direction (*bottom*) with DSC levels 85% (*left*) and 95% (right).

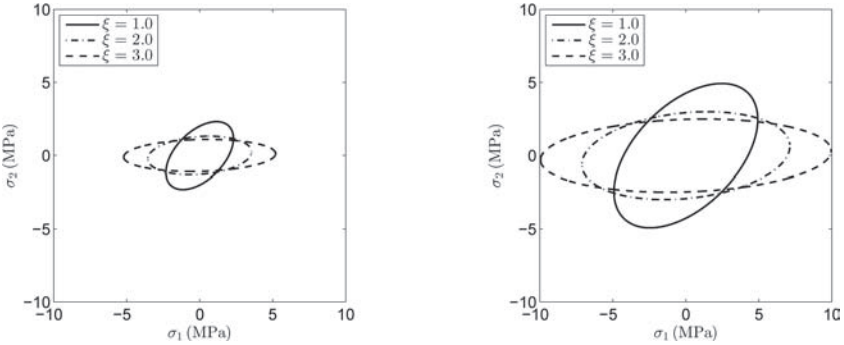

Figure 3. Examples of the initial yield surfaces with $\sigma_{12} = 0$ for anisotropy levels 1.0, 2.0 and 3.0 and DSC levels 85% (*left*) and 95% (*right*).

Step 3: The final constant through-thickness dry solids content (elasto-plastic approach 95% and viscoelastic approach 93%) is applied.

Step 4: External in-plane tensions (if any) are removed.

Step 5: The boundary condition restraining the out-of-plane deformation of the sample is removed. All displacements and rotations are still restrained in the middle of the sample.

Different dry solids content limits were used due to the measurements related to the viscoelastic material model.

The finite element simulations were performed using Abaqus/Standard and shell element S4R [25]. The in-plane size of the element was 3 mm × 3 mm, and in the thickness direction, the element was divided into ten layers of equal thickness, see Figure 7.

2.4 Analytical approach and curl parameters

In the analytical procedure, the inputs are anisotropy ξ, orientation angle θ and plastic strain ε_p. The anisotropy and orientation angle define anisotropy index ϕ according to Eq. (4). The anisotropy index is calculated at 1° intervals, i.e. ϕ = 0°, 1°, 2°, . . ., 359° and it forms, for example, the distributions presented in Figure 8 (top left) for the bottom and the top side anisotropies 2.5 and 2, respectively, and orientation angles 30° and –30°. The hygroexpansion strain distribution corresponding to the given anisotropy ξ and orientation angle θ is determined using Eq. (5) and

$$\varepsilon_h = -\int_{c_0}^{c} \beta \, dc, \tag{7}$$

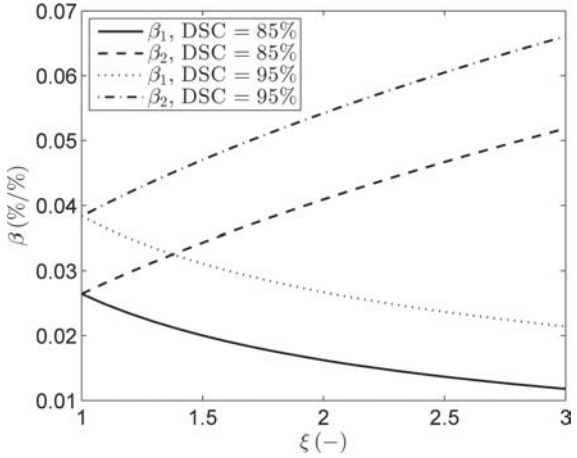

Figure 4. Examples of the moisture expansion coefficients used in the hygro-elasto-plastic approach as a function of the fibre orientation anisotropy for the DSC levels 85% and 95%.

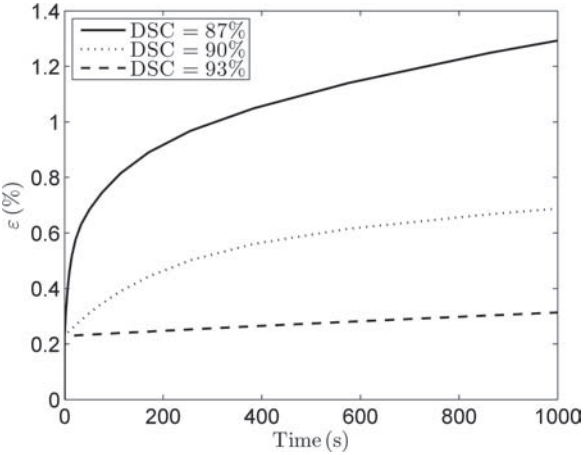

Figure 5. Simulated creep under 30.0 MPa tension.

where c_0 (–) is the reference dry solids content and c is the current dry solids content. Eq. (7) is used when the analytical results are considered with the simulated results obtained by the elasto-plastic material model. When the analytical results are compared with the results obtained by the viscoelastic material model

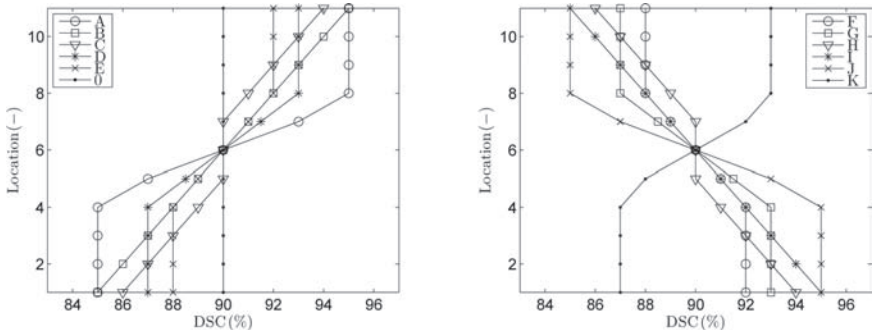

Figure 6. Dry solids content profiles applied with the hygro-elasto-plastic approach (A–K and 0) and hygro-viscoelastic approach (K and 0).

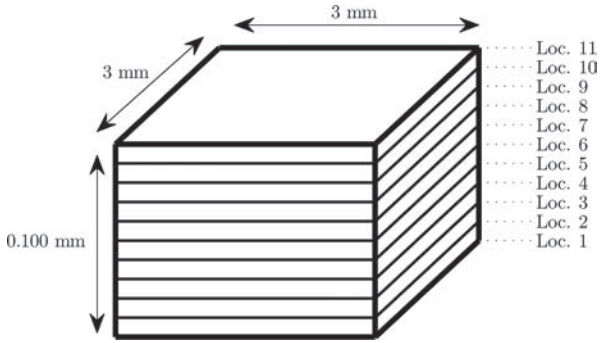

Figure 7. Element used in the simulations. The thickness directional DSC profile is given in the locations 1–11.

as in the example presented in Figure 8, β (Eq. (5)) is determined with the dry solids content $c = 0.90$ and it is independent of the dry solids content. Eq. (7) is thus simplified to

$$\varepsilon_h = -\beta(c - c_0). \tag{8}$$

The measured orientations and applied dry solids content may vary from layer to layer causing also different hygroexpansion and plastic strains to every layer. The average values of strains for the bottom side as well as for the top side are calculated as weighted averages

$$\varepsilon_{BS} = \frac{\sum_{i=1}^{5} \varepsilon_i d_i}{\sum_{i=1}^{5} d_i} \quad \text{and} \quad \varepsilon_{TS} = \frac{\sum_{i=6}^{10} \varepsilon_i d_i}{\sum_{i=6}^{10} d_i}, \tag{9}$$

where d_i is the distance of the layer i from the middle plane.

If the hygroexpansion strain is applied to the circular sheet, the relative deformation distribution of the bottom and the top side in the dry solids content change can be presented as in Figure 8 (top right). The difference between the bottom side and the top side strain is calculated simply by

$$\Delta\varepsilon = \varepsilon_{BS} - \varepsilon_{TS}, \tag{10}$$

and the strain difference may show both positive and negative components, as is seen in Figure 8 (bottom left). As the parameters of the analytical procedure for predicting the curl tendency, the extreme values of $\Delta\varepsilon^+$ and $\Delta\varepsilon^-$ and the angles ω^+ and ω^- of the positive and the negative components of the strain difference distributions are determined. The angles to counterclockwise from the machine direction are defined to be positive. The simulated curl obtained using moisture expansion coefficients and dry solids content change equivalent to those in the analytical approach is presented in Figure 8 (bottom right). The curl results are obtained using the viscoelastic approach with time 10^8 seconds after the step 5 in intention to approximate the elastic solution. The curvature parameters K_{MD}, K_{CD}, and K_{MDCD} are solved by fitting equation

$$K_{MD} \cdot x_{MD}^2 + K_{CD} \cdot x_{CD}^2 + K_{MDCD} \cdot x_{MD} \cdot x_{CD} + a_1 \cdot x_{MD} + a_2 \cdot x_{CD} + a_3 = z, \tag{11}$$

where a_1, a_2 and a_3 are fitting parameters and z is the deviation of the sheet to the out-of-plane direction. The main angle of the curl surface ψ is solved from the equation

$$\psi = \frac{1}{2} \tan^{-1}\left(\frac{K_{MDCD}}{K_{MD} - K_{CD}} \right). \tag{12}$$

$K\psi$ can be determined by applying the coordinate rotation to Eq. (11) using the angle ψ.

In the example in Figure 8, the negative $\Delta\varepsilon^-_h$ has a higher extreme value than $\Delta\varepsilon^+_h$. This implies a curl mode in which the edges of the sample are bend towards the BS approximately in the direction $\omega^- = -46°$. The main angle ψ of the simulated

curl is approximately perpendicular to ω^- indicating analogy between the analytical approach and the numerical method in this simple example even though the stiffness is not included in the analytical approach.

3 RESULTS

The structure based curl tendency is studied using artificial orientation structures via the analytical approach and viscoelastic simulations in Figures 9–12. The equal anisotropy $\xi_{TS} = 2$ and fibre orientation angle $\theta_{TS} = 0°$ was set to all top side layers 6 to 10. For bottom side layers 1 to 5, the anisotropies $\xi_{BS} = 1.5$ in Figure 9, $\xi_{BS} = 2.0$ in Figure 10 and $\xi_{BS} = 2.5$ in Figure 11 are used in the simulations with alternative fibre orientation angle θ_{BS} values: 1°, 5°, 10°, 30°, 45° or 80°. The corresponding hygroexpansion distributions were calculated for both sides assuming the dry solids content change from 87% to 93%. In the simulations, the dry solids content profile was 0 (Figure 6) and no in-plane tensions were applied during simulations. The results were gathered 10^8 seconds after the sheet was released, i.e., the result approximates the elastic response. In Figure 10, where the anisotropies of the both sides of sheet are equal, the negative and positive components of the strain differences $\Delta\varepsilon_h$ are equivalent. Because both components have an equivalent effect on the curl tendency, the saddle mode of the curl appears in simulated results. It should be noted that the difference of the directions of the main components ω^+ and ω^- is not 90 degrees. In Figures 9 and 11, the difference in anisotropies between the two sides of the sheet cause the intensity difference between $\Delta\varepsilon_h$ components and the simulated curl produces a virtually cylindrical shape; however, the change of the main axis of the curl ψ caused by the change of the bottom side orientation angle θ_{BS} is not trivial. The behaviour of the angles and intensities of the strain differences of the analytical approach are presented for $\theta_{BS} = [1° : 90°]$ in Figure 12. The curvature $K\psi$ and perpendicular value of the main angle of curl $\psi_\perp$ produced by numerical simulations are also marked, indicating the good correspondence between the methods.

Figure 13 shows the simulated time-dependent curl and corresponding curl obtained with the elasto-plastic approach when the dry solids content profile K (Figure 6) was applied to the sample. A homogeneous MD orientated structure ($\theta_{TS} = \theta_{BS} = 0°$, $\xi_{TS} = \xi_{BS} = 2.0$) was established and no in-plane tensions were applied to the sheet during simulations. In viscoelastic simulations, the effect of time that is prevailing during the through-thickness dry solids content profile has a significant effect on the curvature. On the other hand, the recovery of curl can be observed in a released sheet curvature approaching approximately the elastic solution. In this exemplary case, the elasto-plastic simulation gives curvature which corresponds to the process steps times of 0.6 seconds, or one second process

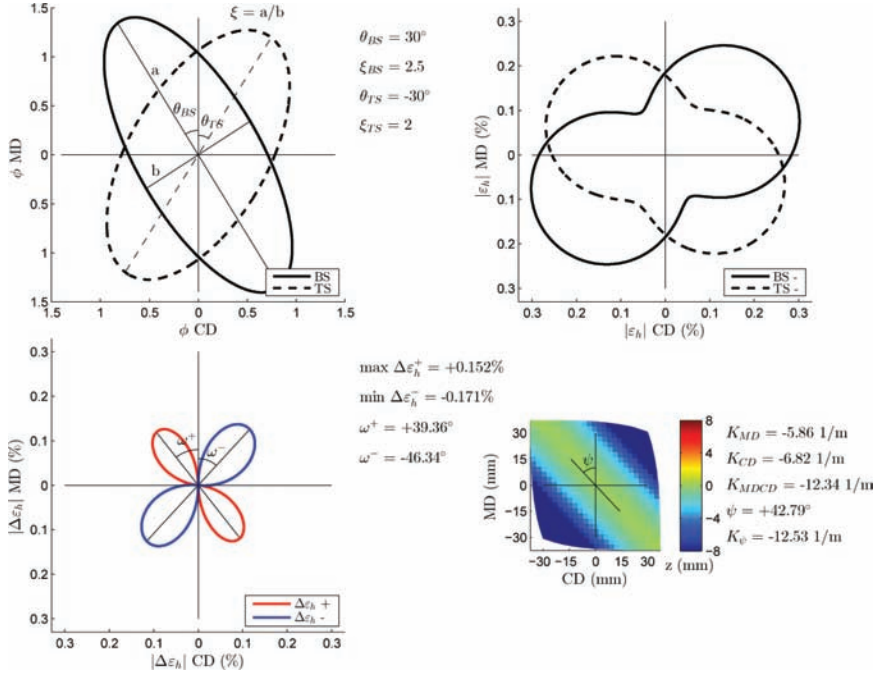

Figure 8. The bottom side (BS) and the top side (TS) anisotropy index distributions (*top-left*) and the corresponding relative hygroexpansion strain distributions (*top-right*), hygroexpansion strain difference between BS and TS (*bottom-left*) and simulated curl viewed from the top side (*bottom-right*).

steps with about a half an hour recovery time. The predicted curl mode caused by the DSC profile is quantitatively similar between the viscoelastic and elasto-plastic approach, although the material model related mechanism to produce curl due to the DSC profile is fundamentally dissimilar.

In the elasto-plastic simulations, the external tension or DSC profiles may introduce plastic deformations to the sample, and the strain difference tendency of the bottom and top side is no longer defined only by hygroexpansion strains. Figure 14 demonstrates the effect of the plastic strain component on the curl magnitude and mode when the dry solids content profile H is applied during hygro-elasto-plastic simulation without external tensions. Again, the artificial orientation structure was set with $\xi_{TS} = 2.0$ and $\theta_{TS} = 0$. The orientation structure parameters of the bottom side are presented besides the strain difference figures. In the elasto-plastic simulation, the DSC change is from 85% to 95% and the dry solids content dependent moisture expansion coefficient is used according to Eq. (5). In the uppermost and

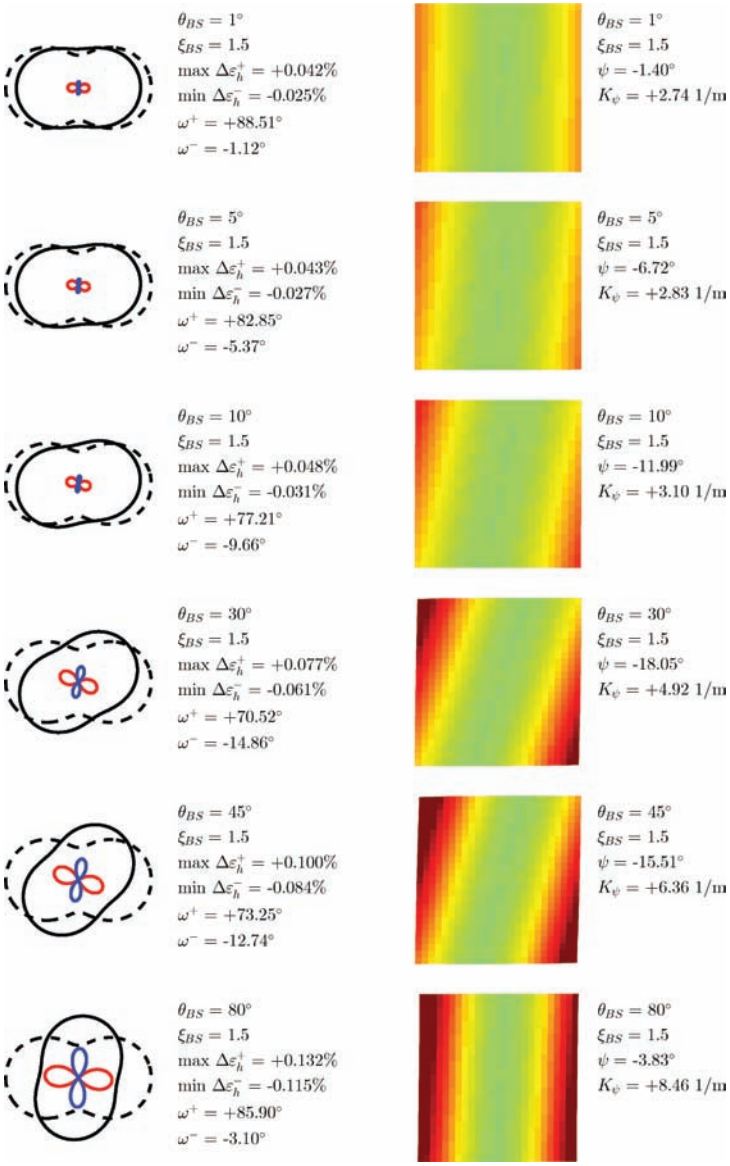

Figure 9. Hygroexpansion strain distributions and the difference between the bottom side and the top side (*left*) and the simulated curl (*right*). $\xi_{BS} = 1.5$, $\xi_{TS} = 2.0$ and $\theta_{TS} = 0$ while θ_{BS} varies. For the axes, scales and definitions, see Figure 8.

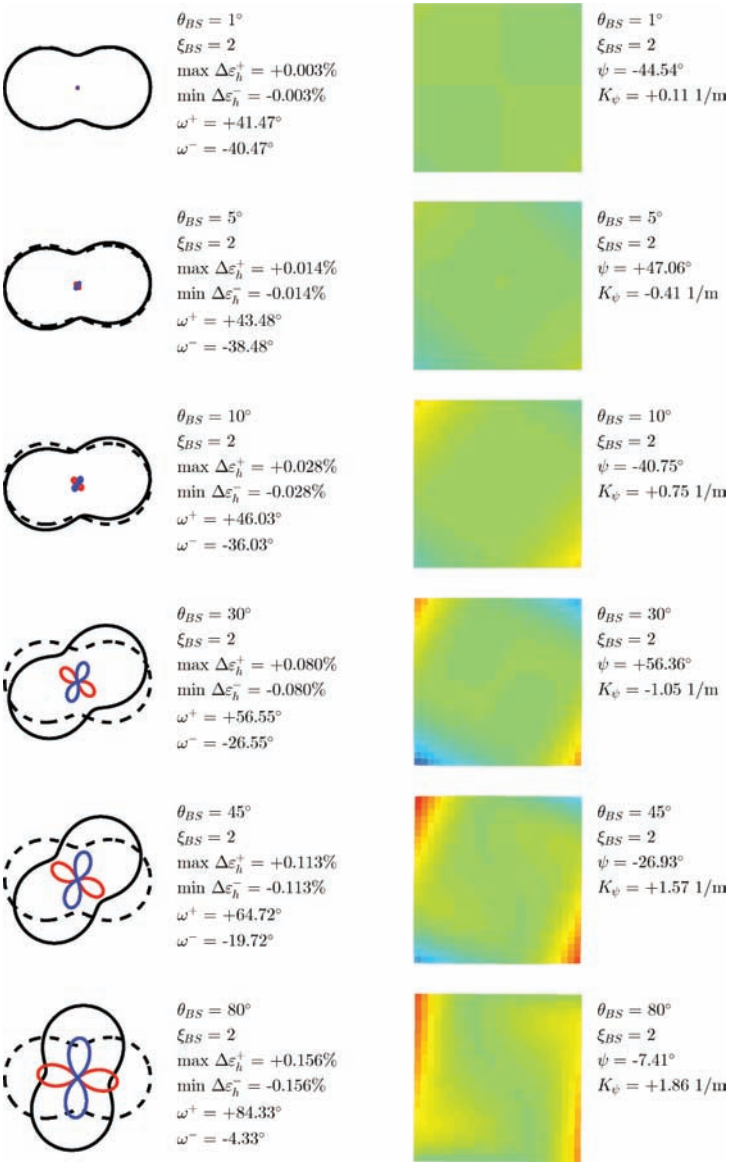

Figure 10. Hygroexpansion strain distributions and the difference between the bottom side and the top side (*left*) and the simulated curl (*right*). $\xi_{BS} = 2.0$, $\xi_{TS} = 2.0$ and $\theta_{TS} = 0$ while θ_{BS} varies. For the axes, scales and definitions, see Figure 8.

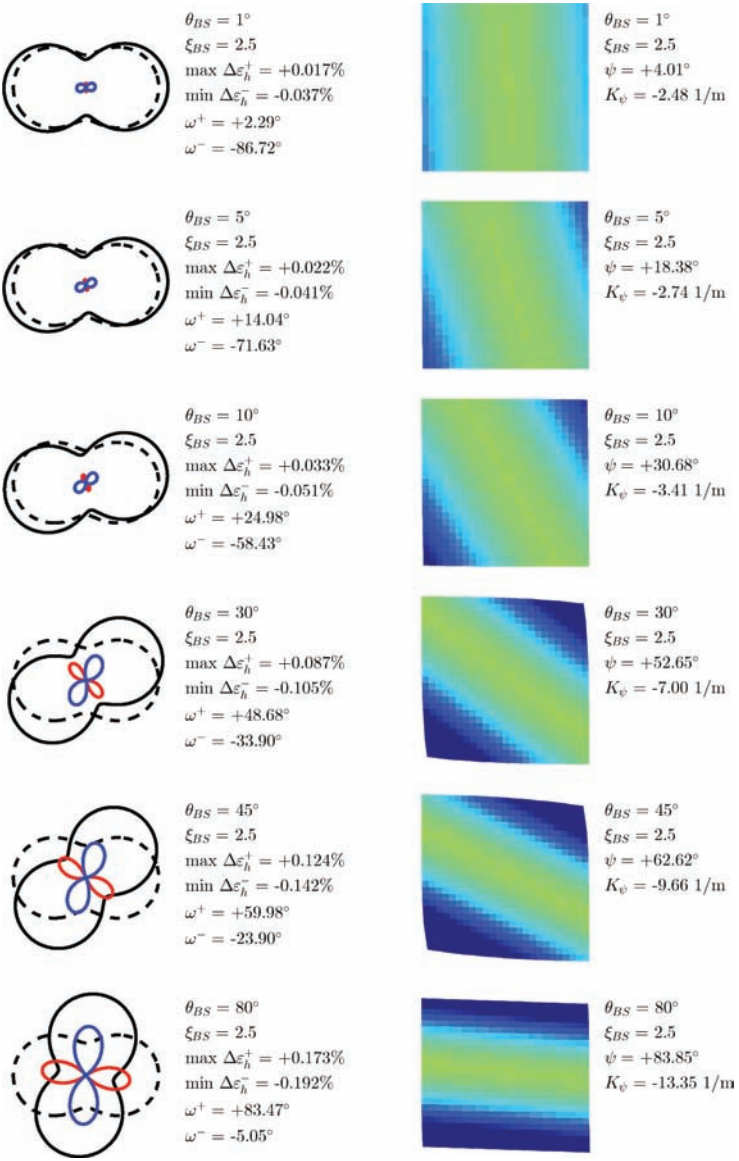

Figure 11. Hygroexpansion strain distributions and the difference between the bottom side and the top side (*left*) and the simulated curl (*right*). $\xi_{BS} = 2.5$, $\xi_{TS} = 2.0$ and $\theta_{TS} = 0$ while θ_{BS} varies. For the axes, scales and definitions, see Figure 8.

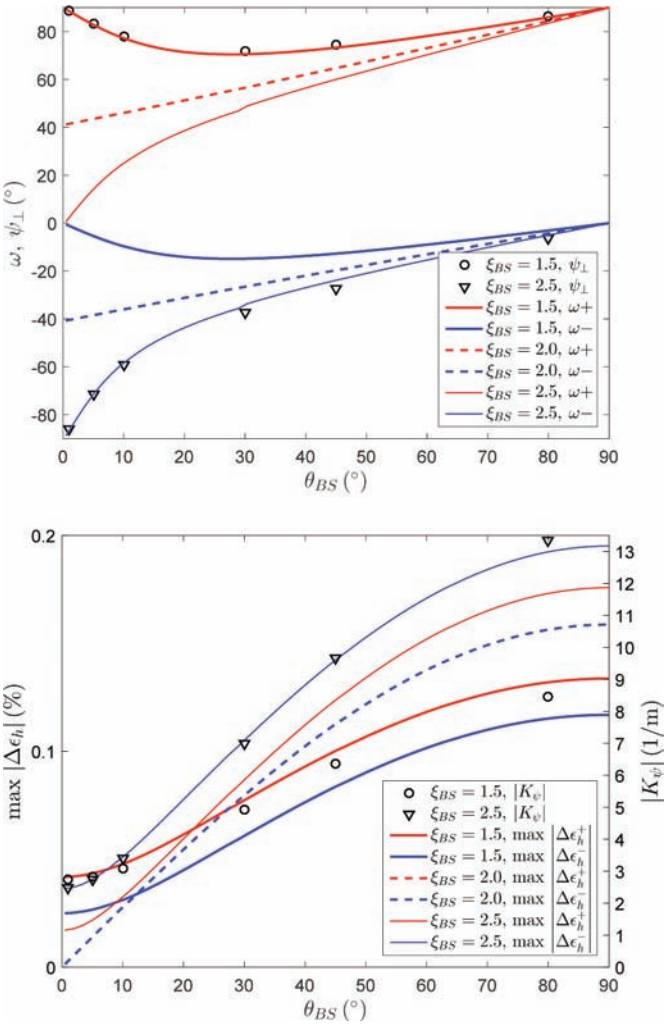

Figure 12. Angles (*top*) and amplitudes (*bottom*) of strain difference components determined using the analytical approach (lines) and from the viscoelastic simulations (markers).

second from the bottom figures in Figure 14, DSC profile was 0 and no plastic strains are induced during the simulations. In the second from the top and bottom figures in Figure 14, the DSC profile H is applied and plastic strains appear during numerical simulations on layers 1, 9 and 10. The plastic strains for the second case from the top are for the bottom side MD 0.0013% and CD 0.0028% and for top

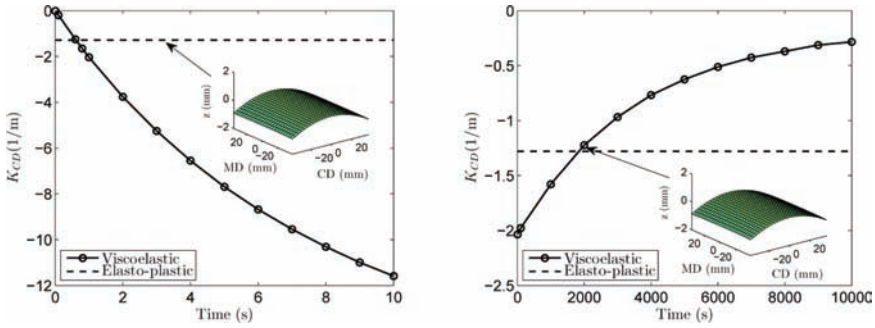

Figure 13. Curvature as a function of the step duration (*left*). Identical step duration is used in all five steps. Curvature attenuation after the sheet is released (*right*). The duration is one second for all five steps.

side MD and CD –0.0044% and –0.0227%, respectively. For the sample at the bottom, the corresponding values are 0.0015%, 0.0083%, –0.0044% and –0.0269%. These plastic strains are summed up to analytical hygroexpansion strain distributions resulting in deformed strain difference distributions. The intensity and direction of strain difference components may undergo changes and the dominating strain difference component may be switched.

The analytical approach and numerical simulations using the elasto-plastic material model can be applied to measured structures presented in Figure 1. The dry solids content change from 85% to 95% with the DSC profile 0 and without external tensions applied to measured structures produced the strain distributions, strain difference distributions and curl topographies presented in Figure 15. The results show the fibre orientation structural based hygroexpansion strain and its effect on curl. The significant difference in anisotropy between the two sheet sides leads to a higher curl magnitude. High oriented shear during the forming of Samples 2, 6 and 7 has produced symmetric structures with a low magnitude of curvature, however, not guaranteeing the zero main axis of curl tendency. Sample 5, having the lowest anisotropy level, has a low magnitude of curvature and only moderate deformation of the main axis of curl from the MD, although the orientation angle difference of the top and bottom side is the largest of these seven samples. The similarity of the predicted curl mode compared to the analytical and elasto-plastic approach is clear even though the elasto-plastic approach includes orthotropic in-plane stiffness varying through thickness.

The through-thickness dry solids content profiles presented in Figure 6 were applied to the measured structures (Figure 1) together with different in-plane tension conditions using elasto-plastic approach. The tension applied to the MD

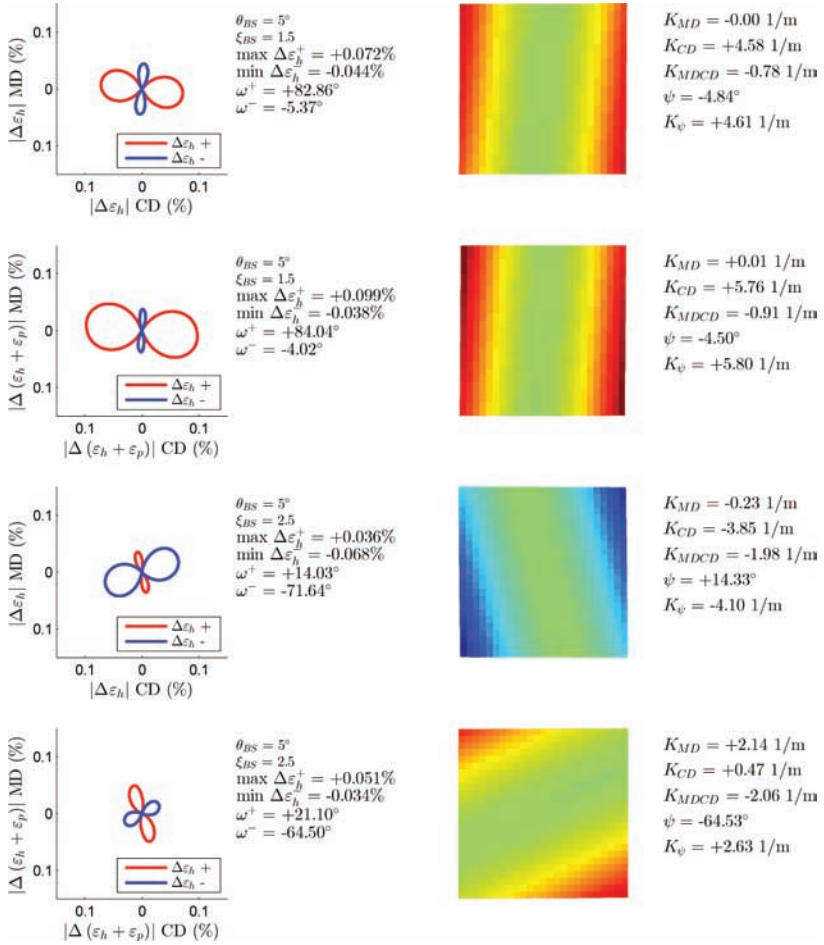

Figure 14. Strain difference distribution (*left*) and corresponding simulated curl (*right*). The top side anisotropy and orientation angle are $\xi_{TS} = 2.0$ and $\theta_{TS} = 0$. For the axes, scales and definitions not shown, see Figure 8.

and CD are 0 N/m, 200 N/m, 400 N/m, and 600 N/m, and a total of 176 combinations of simulation conditions were applied to each sample. An example of the effect of the simulation conditions on the curl tendency of the structure of Sample 4 is presented in Figure 16 in a situation where the MD tension is constantly 200 N/m. The effect of all input combinations of DSC profiles and CD tensions on curl parameters are illustrated as surfaces. For the structure of Sample 4, there is a clear discontinuity front, where the curl tendency changes from a negative

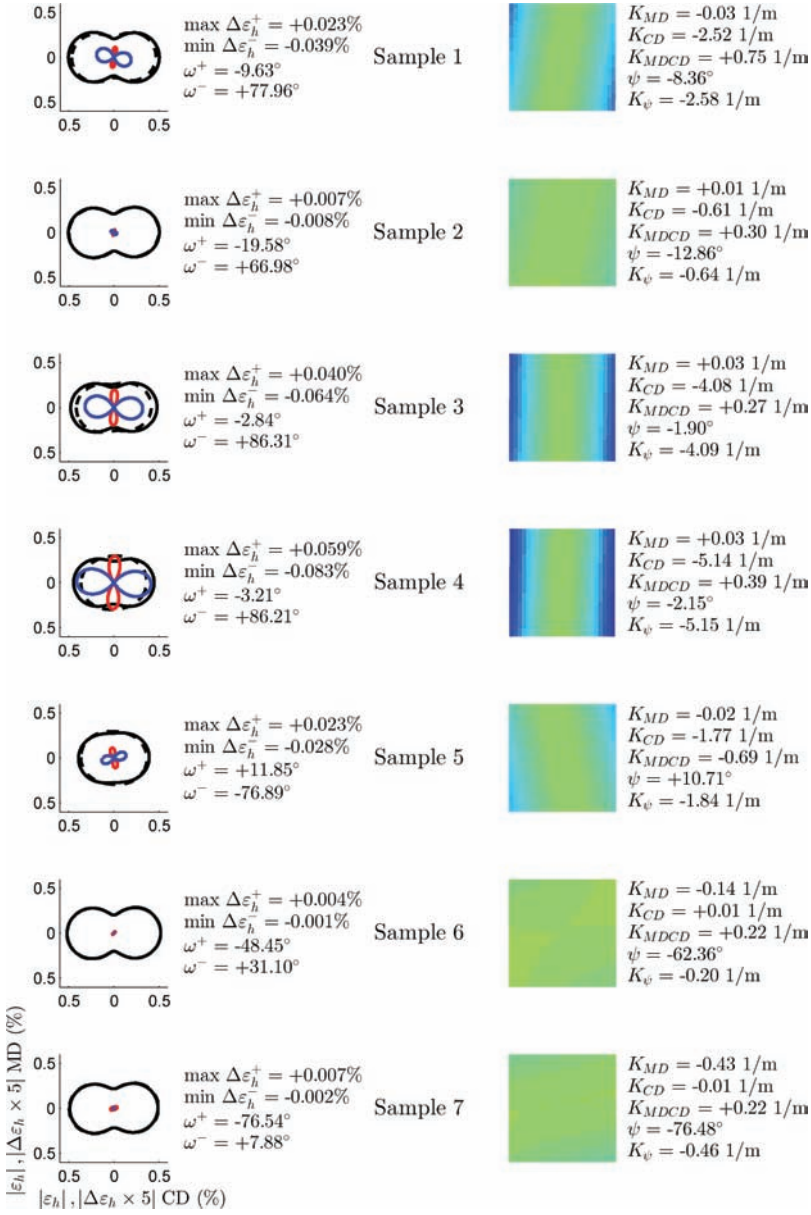

Figure 15. Hygroexpansion strain distributions and the difference between the bottom side and the top side (*left*) and simulated curl (*right*) of the measured samples. For the axes, scales and definitions not shown, see Figure 8.

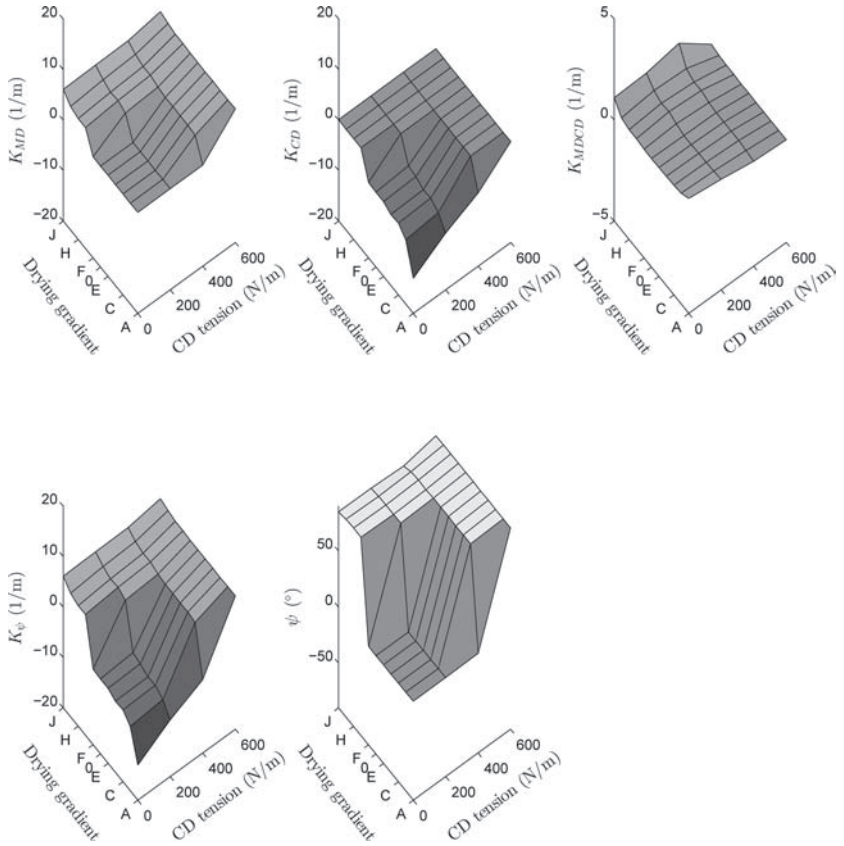

Figure 16. Curvature parameters of Sample 4 as a function of the DSC profile and CD tension. Constant MD tension 200 N/m.

component to a positive component, i.e., the curvature changes from a negative to positive and the main angle of curl changes approximately 90°. Both tension conditions and DSC profiles are effective parameters in this change. The effect of these parameters also depends on the paper structure and is not always as systematic as for Sample 4, which can be seen from examples of Samples 1 and 5 in Figure 17.

The exposure of the sheet to a thermal pulse of fuser in photocopying or printing process can cause it to curl. The high magnitude of curl as well as CD curl (curl main axis along the CD) and diagonal modes are the most troublesome, resulting in paper jams in copiers or printers. If the simulated curl tendency with DSC profile 0 and no external tensions, i.e. a purely structural based curl tendency, is

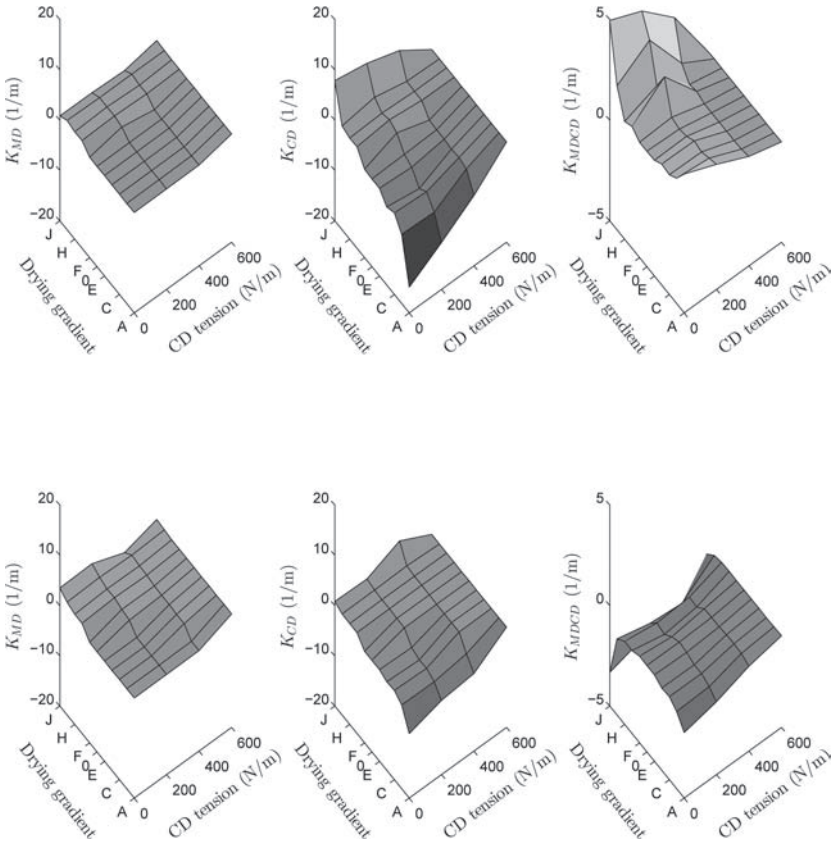

Figure 17. Curvature parameters of Samples 1 (*top*) and 5 (*bottom*) as a function of the DSC profile and CD tension. Constant MD tension 200 N/m.

compared with the measured curl induced by photocopier process, no clear correlation between results can be obtained; see Figure 18 (left). The correlations between curvatures obtained using different combinations of DSC profile and external tensions in simulations and measured curvatures were calculated. The assumption is that very simple simulation steps are able to combine the manufacturing and photocopying conditions effective for curl. In this study, only a rough preliminary optimization approach is used; the best combinations of DSC profile and tensions for predicting of measured curl induced by photocopying (and drying) is selected from the set of simulations using correlation coefficient as criterion. The maximum correlation r = 0.95 for the measured curl after bottom side copying was achieved with DSC profile B, MD tension 400 N/m and CD

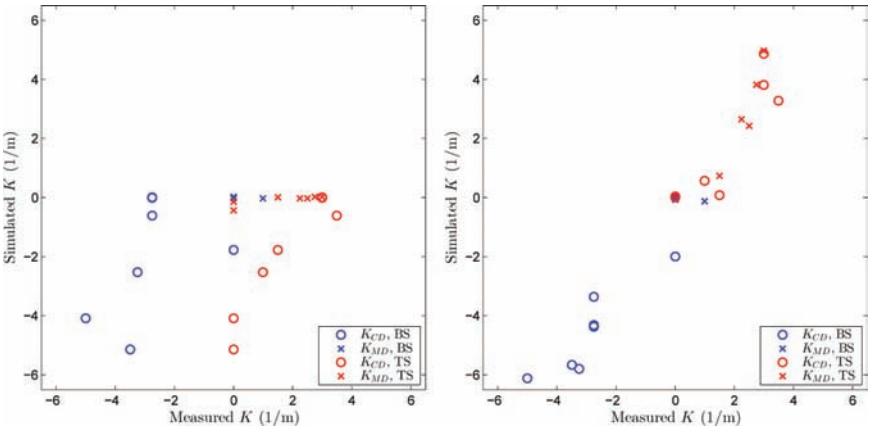

Figure 18. Correlations between the measured and simulated curl. Simulation conditions: DSC profile 0, MD tension 0 N/m, CD tension 0 N/m (BS and TS) (*left*), DSC profile B, MD tension 400 N/m, CD tension 0 N/m (BS) (right) and DSC profile I, MD tension 600 N/m, CD tension 200 N/m (TS) (*right*).

tension 0 N/m. For top side copying, the maximum correlation r = 0.90 was achieved with DSC profile I, MD tension 600 N/m and CD tension 200 N/m. The results related to the maximum correlations are presented in Figure 18 (right). The measured K_{MD} and K_{CD} and corresponding simulated curls are presented in Figure. 19. A comparison of the structure (Figure 1), the structure based curl (Figure. 15) and curl induced by photocopying process in the production machine samples proves that the detection of the curl mode from the orientation structure is not obvious or straightforward; e.g. the orientation structure of Samples 2, 6 and 7 are almost equivalent, yet Sample 2 introduces clearly a diagonal curl mode in top side copying according to both measured and simulated results. Overall, very minor orientation angle differences between sides may introduce diagonal curl and a CD curl mode in some specific conditions. However, the results indicate that a complicated drying process with a consecutive copying process comprising different temperature and dry solids content profiles as well as external tensions can be imitated by integrating it into a few simple simulation steps.

4 DISCUSSION AND CONCLUSIONS

All three approaches presented in this paper – analytical, hygro-viscoelastic and hygro-elasto-plastic – are useful for predicting the curl mode or magnitude in specific applications. The strain difference distributions produced by the analytical

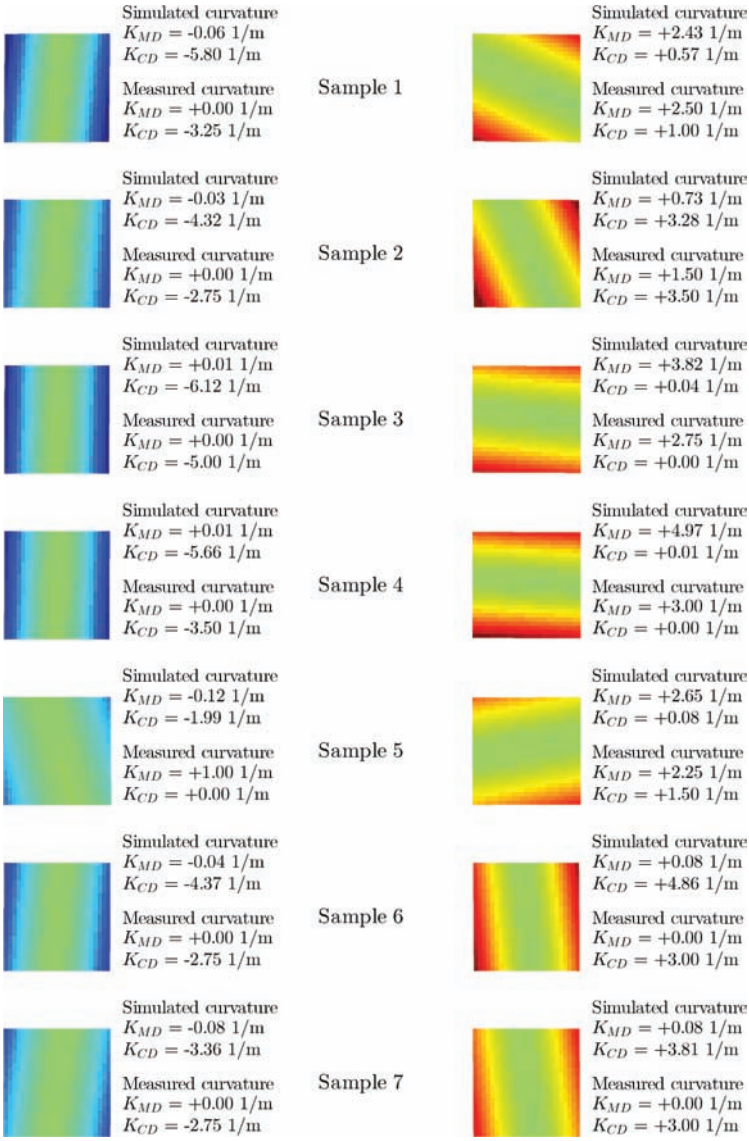

Figure 19. Simulated curls obtained with equivalent simulation conditions as in Figure 18 (*right*). Bottom side copying (*left*) and top side copying (*right*). For the axes and scales see Figure 8.

approach demonstrate the determination of the curl mode and magnitude. For optimising favourable paper curl behaviour, the analytical approach provides computational efficiency for structural design of paper or board fibre orientation. In some simple cases, plastic deformations can also be solved analytically from the elasto-plastic material model (see e.g. [21]). However, managing the complexity of emerging permanent strain at different layers of a sample when drying, DSC profiles and tensions in different directions prevail simultaneously require utilizing of numerical methods. Hygro-viscoelastic and hygro-elasto-plastic approaches provide different means of predicting the effect of dwell times and lags, external tensions and through-thickness dry solids content differences during paper making and converting processes on curl mode and magnitude. In specific cases, both simulation approaches presented in this study produce almost equivalent results. The results obtained by the viscoelastic simulations always approach the elastic solution when the attenuation time increases. Furthermore, if the aim is to study the permanent manifestation of curl form induced in the paper sheet by thermal or moisture changes or the mechanical processing of sheet, the plastic component of the material model is valuable.

The prediction of the curl tendency (the curl magnitude and mode) induced by photocopier process is a challenging task. First of all, the structure of the sheet as well as drying conditions and storage have an effect on the curl tendency. Moreover, the thermal properties of the sheet are strongly affected by the moisture content, basis weight, density, thermal conductivity and heat capacity [26] and also the temperature, moisture and pressure fields in a sheet during traveling thermal pulse are strongly dependent on the sheet properties [27]. In any case, intense through-thickness dry solids content gradients may appear in a sheet during one-sided heating [28]. Simulating all process steps consecutively with appropriate dwell times would require a huge number of measurement parameters related to process conditions and transport, material and structural properties of a sample. Also the behaviour of plastic deformations (or time parameters) in consecutive process steps in elasto-plastic (or viscoelastic) material models is questionable [29]. The simple drying processes including a through-thickness dry solids content profile presented in Figure 6 and external in-plane tension in MD and CD were assumed to include both the effects of the drying and the copying processes. The only structural information used in simulations was sheet thickness and layered fibre orientation. Exceptionally good correlations with curl magnitude and curl mode were achieved for specific drying combinations. This result implies that hygro-elasto-plastic simulations with only a few simulation steps can be calibrated to estimate a complex consecutive process entity, and the structure can then be optimised by this calibrated simulation process. The connected process sets can at least partly be considered as a black box. Validity of a “process-tailored” model of this type is not guaranteed for different process

combinations and development of optimisation procedure needs more test cases. In any case, the prediction of the curl mode was proven to be non-trivial, and simulation tools are essential.

ACKNOWLEDGEMENTS

The simulations were performed by the commercial software Abaqus, which was licensed to CSC (the Finnish IT Center for Science).

REFERENCES

1. S. F. Smith. Dried-in strains in paper sheets and their relation to curling, cockling and other phenomena. *The Paper-Maker and British Paper Trade Journal* **119**:185–192, 1950.
2. P. Glynn, H. W. H. Jones and W. Gallay. The fundamentals of curl in paper. *Pulp and Paper Magazine of Canada* **60**:316–323, 1959.
3. W. Gallay. Stability of dimensions and form of paper. *Tappi* **56**:90–95, 1973.
4. L. Carlsson, C. Fellers and M. Htun. Curl and two-sidedness of paper. *Svensk Papperstidning* **83**:194–197, 1980.
5. L. Carlsson. Out-of-plane hygroinstability of multi-ply paperboard. *Fiber Science and Technology* **14**(3):201–212, 1981.
6. T. Leppänen and J. Hämäläinen. Effect of local curls on the cockling of paper. *Nordic Pulp and Paper Research Journal* **22**(1):72–75, 2007.
7. T. Uesaka, I. Kodaka, S. Okushima and R. Fukuchi. History-dependent dimensional stability of paper. *Rheologica Acta* **28**:238–245, 1989.
8. W. Lu and L. Carlsson. Influence of viscoelastic behavior on curl of paper. *Mechanics of Time-Dependent Materials* **5**:79–100, 2001.
9. L.-E. Eriksson, S. Cavlin, C. Fellers and L. Carlsson. Curl and twist of paper-board – theory and measurements. *Nordic Pulp and Paper Research Journal* **2**(2):66–70, 1987.
10. J. Decker, A. Khaja, M. Hoang, J. Considine, D. Vahey, K. Turner and R. Rowlands. Variation of paper curl due to fiber orientation. In proc. *The SEM Annual Conference*, pp. 347–352, Indianapolis, USA, 2010.
11. P. Viitaharju and K. Niskanen. Chiral curl in thin papers. *Journal of Pulp and Paper Science* **20**(5):148–152, 1994.
12. W. Lu and L. Carlsson. Influence of initial deflections on curl of paper. *Journal of Pulp and Paper Science* **27**:373–379, 2001.
13. U. Hirn and W. Bauer. Investigating paper curl by sheet splitting. In proc. *EUCEPA Conference 'Challenges 06=': Challenges of Pulp and Papermaking Technology*, pp. 1–18, Bratislava, Slovak, 2006.
14. G. Bortolin, P.O. Gutman and B. Nilsson. On modelling of curl in multi-ply paperboard. *Journal of Process Control* **16**:419–429, 2006.

15. T. Sasaki, H. Sano, J. Yamamoto, H. Todoroki, K. Ono and T. Ochi. On-line fiber orientation measurement and control. *Pulp and Paper Canada* **111**(2):35–39, 2010.
16. R. Pietikäinen and M. Kurki. Simulation of the paper sheet curling. In *Proceedings of 5th Finnish Mechanics Days*, pp. 257–264, Jyväskylä, Finland, 1994.
17. P. Lipponen, A.-L. Erkkilä,, T. Leppänen and J. Hämäläinen. On the importance of in-plane shrinkage and through-thickness moisture gradient during drying on cockling and curling phenomena. In *Advances in Pulp and Paper Research, Transactions of the 14th Fundamental Research Symposium*, (ed. S. J. I'Anson), pp. 389–436, FRC, Oxford, UK, 2009.
18. A.-L. Erkkilä, T. Leppänen and T. Tuovinen. The curl and fluting of paper: the effect of elasto-plasticity. In proc. *The VII European Congress on Computational Methods in Applied Sciences and Engineering*, pp. 4752–4769, Crete, Greece, 2016.
19. A.-L. Erkkilä, P. Pakarinen and M. Odell. Sheet forming studies using layered orientation analysis. *Pulp and Paper Canada* **99**(1):81–85, 1998.
20. A.-L. Erkkilä, P. Pakarinen and M. Odell. The effect of forming mechanisms on layered fiber structure in roll and blade gap forming. In proc. *TAPPI 99–Preparing for the Next Millennium*, pp. 389–400, Atlanta, USA, 1999.
21. A.-L. Erkkilä, T. Leppänen, J. Hämäläinen and T. Tuovinen. Hygro-elasto-plastic model for planar orthotropic material. *International Journal of Solids and Structures* **62**:66–80, 2015.
22. A.-L. Erkkilä, T. Leppänen and J. Hämäläinen. Empirical plasticity models applied for paper sheets having different anisotropy and dry solids content levels. *International Journal of Solids and Structures* **50**:2151–2179, 2013.
23. A.-L. Erkkilä, T. Leppänen, M. Ora, T. Tuovinen and A. Puurtinen. Hygroexpansivity of anisotropic sheets. *Nordic Pulp and Paper Research Journal* **30**:325–334, 2015.
24. J. Sorvari, T. Leppänen and J. Silvennoinen. The effect of inhomogeneous hygroexpansion on the moisture accelerated creep of paperboard. Submitted to *International Journal of Solids and Structures*, 2017.
25. Abaqus documentation. Dassault Systèmes, Providence, USA, 2013.
26. S. Lavrykov, B. Ramarao, R. Solimeno, K. Singh. Analysis of heat and moisture transients in paper during copying and digital printing processes. *Journal of Imaging Science and Technology* **57**(6):060504-1-060504-8, 2013.
27. A. Bandyopadhyay, B. Ramarao, E. Shih. Transient response of a paper sheet subjected to a traveling thermal pulse: evolution of temperature, moisture and pressure fields. *Journal of Imaging Science and Technology* **45**(6):598–608, 2001.
28. S. Oohara, Y. Hayama, H. Tanigawa, T. Tsuruta. Analysis of the paper curl amount in the fusing process of electrophotography by calculation of moisture transport. In proc. *NIP28: 28th International Conference on Digital Printing Technologies & Digital Fabrication Conference*, pp. 289–293, Quebec City, Canada, 2012.
29. T. Leppänen, A.-L. Erkkilä, J. Kouko, V. Laine and J. Sorvari. A plasticity model for predicting the rheological behavior of paperboard. *International Journal of Solids and Structures* **106–107**:38–45, 2017.

Transcription of Discussion

PREDICTION OF CURLING BEHAVIOUR

A.-L. Erkkilä,[1] *T. Leppänen,*[2] *J. Sorvari*[3] *and T. Tuovinen*[1]

[1] University of Jyväskylä, P.O. Box 35, FI-40014 Jyväskylä, Finland
[2] LUT Savo Sustainable Technologies, Lappeenranta University of Technology, Varkaus Unit, Opiskelijankatu 3, FI-78210 Varkaus, Finland
[3] Centre of Computational Engineering and Integrated Design (CEID), Lappeenranta University of Technology, P.O. Box 20, FI-53851 Lappeenranta, Finland

Ulrich Hirn Graz University of Technology

I think when developing the mode of curl that is eventually showing up in the copier, it is extremely important to consider the pre-deformation of the paper because in the printer there is a roll system where the paper is transported. So essentially we have somewhat of a pre-deformation before printing. I think you really need to consider this when modelling the final curl developing in the copying process.

Anna-Leena Erkkilä University of Jyväskylä

Yes, that's true. There are many factors affecting curl tendency, for example, porosity, thermal conductivity and mechanical response of sheet. Secondly, if we think this kind of elasto-plastic material model and hardening model, isotropic, kinematic or any kind; is it possible to apply several consecutive process steps and still correctly retain the history of previous steps? In contrast to the approach, where all paper properties and external conditions during processes have been pursued to simulate in detail, in this study, only a few simple simulation steps have been used to integrate all that. Roughly speaking, all processes have been integrated in that one step, which introduces dry solids content profile with prevailing tensions during drying and then this has been optimized to estimate complex process combination including different conditions during manufacturing and in mechanical and thermal handling of the copying process.

Discussion

Ulrich Hirn

The point I am trying to make is, if you have a pre-deformation in MD you need to overcome this pre-deformation for instance to get a CD curl and the degree of the pre-deformation that you have depends on the copying machine. It's not only a factor of the sheet and the moisture gradient, it's also a factor of the converting and the printing process itself and that would also be worthwhile to include.

Anna-Leena Erkkilä

Yes, that's true. Here the optimization for bottom and top side copying were done only for those specific process combinations, but anyway, this is an example that it is possible to do. Therefore, if there is different copying process and different paper machine, a new optimization may have to be done.

Ron Peerlings Eindhoven University of Technology

I didn't quite get the viscoelastic model that you were using. Is it a linear viscoelastic model and how does the moisture content, or humidity enter in the viscoelasticity?

Anna-Leena Erkkilä

There is a typing error in Equation (6). The creep compliance matrix D should be a function of the reduced time Ψ and not a function of time, i.e. Equation (6) should be

$$\varepsilon(t) = \int_0^t D(\psi(t) - \psi(\tau))\dot{\sigma}(\tau)\, d\tau + \beta\Delta c.$$

The reduced time is an integral

$$\psi(t) = \int_0^t \frac{d\eta}{a(c(\eta))}$$

where the time-shift parameter a is a function of the moisture content c. This is standard way of including moisture, or temperature, into integral based viscoelastic models. The more detailed description will be presented in the submitted paper: J. Sorvari, T. Leppänen and J. Silvennoinen. "The effect of inhomogeneous hygroexpansion on the moisture accelerated creep of paperboard."

Tetsu Uesaka Mid Sweden University

I am just wondering, did you consider so called bifurcation phenomena? What we call, "Flip curl". Suppose you have a piece of copy paper. When you flip it, you change the curl axis in the direction x on y and so on. Every paper has a kind of potentially different curl shape depending on the size, the dimension, and geometry. Therefore, what you see is different from what you calculated as a curvature. Have you considered this?

Anna-Leena Erkkilä

I am not sure, if I understood correctly your question, but at least, there is usually those two modes of strain differences as is illustrated in the example in Figure 8. If they are almost equal in magnitude, the sheet can easily change the curl mode due to some impulse.

Tetsu Uesaka

Yes, that is the case, but whether it showed up or not, it depends on the dimensions and the geometry.

Anna-Leena Erkkilä

Yes, that is true also.

Tetsu Uesaka

And it also depends on the path you took to reach that point. This is a path-dependent phenomenon, so it is tricky.

Anna-Leena Erkkilä

Yes. The example of effect of the shape of the sheet is demonstrated in Figure 10, where the anisotropies are equal in the bottom and top side of the sheet and then the strain difference modes are equal and curl tendency is toward a saddle-shaped surface. When the main axis of curl is along machine or cross direction, the stiffness of sheet prevents the appearance of saddle-shaped curl, but if the axis of curl is diagonal, the corners can easily bend toward different sides of sheet and saddle-shaped behaviour can be detected even though the curl tendency is equal in these examples.

Discussion

Petri Mäkelä BillerudKorsnas AB

You use dry solids content to keep track of moisture in your work. Is there any particular reason for choosing dry solids content?

Anna-Leena Erkkilä

This is for historical reasons. This is something that we chose long ago and we have continued to use it since.

Petri Mäkelä

I am a bit worried that you build in artificial non-Linearity into modelling by this choice, since the dry solids content is non-linearly related to the weight of moisture in the sheet.

Anna-Leena Erkkilä

The fittings of material parameters and moisture expansion are based on experimental data, where the dry solids content is used as a variable in the derivation of relationships. By a simple change of variable, the material model expressed by Equation (3) and moisture expansion coefficient expressed by Equation (5) can be written to depend for example on moisture ratio. Certainly, the relationship between material parameters and moisture expansion coefficients would look different when plotted as a function of moisture ratio rather than of dry solids content, but still there is equivalent dependence of material parameters and moisture expansion on moisture or dryness. It does not matter which variable is used if you are consistent in using one variable in every step of fitting to experimental data and in the simulations.